SCIENTIFIC COMMITTEE
TWENTY-FIRST REGULAR SESSION

Nuku'alofa, Tonga
13-21 August 2025

Analysis of swordfish CPUE from the Spanish fleet in the Southwest Pacific Ocean

WCPFC-SC21-2025/SA-IP-12
01 August 2025

K. Kim[1], **A. Magnusson**[1], **P. Hamer**[1]

[1]Oceanic Fisheries Programme of the Pacific Community

Table of contents

Executive Summary

This analysis presents updated standardized CPUE indices for swordfish caught by Spanish longline fleets in the Southwest Pacific Ocean (2004-2023), exploring alternative modeling approaches and cross-platform validation.

The base model replicated SC17's delta-gamma structure to maintain continuity. Three exploratory models using Tweedie distributions were developed (M1, M2, and M3): M1 used the same covariates as SC17, M2 added blue shark catch proportion as a species interaction affecting catchability, and M3 incorporated sea surface temperature. These exploratory models were validated across VAST, sdmTMB, and tinyVAST platforms, producing identical results.

M3 showed the best diagnostic performance, while M2 had the lowest AIC but exhibited systematic residual patterns. M1 showed similarly good residuals as M3 but higher AIC. Tweedie models proved more robust than delta-gamma approaches for this dataset with minimal zero catches (0.5%) and showed improved residual patterns compared to the base model. However, all models including the SC17 base showed similar trend patterns and failed to explain recent sharp CPUE declines.

With no substantial differences in trends and Tweedie models being additional exploration, we maintained the SC17 base model, though we recommend Tweedie distributions for future use given their improved robustness and residual patterns. The cross-platform validation confirmed that VAST, sdmTMB, and tinyVAST produce equivalent results, supporting future platform transitions. Future improvements will require better data on longline targeting behavior to develop more reliable abundance indices.

1 Introduction

Standardized catch-per-unit-effort (CPUE) indices provide essential data for fisheries stock assessments by tracking relative abundance trends over time (Maunder & Punt, 2004). Modern geostatistical approaches using spatiotemporal models have substantially improved CPUE standardization by accounting for spatial and temporal variability in fisheries data (Thorson et al., 2015; Thorson, 2019). This paper presents an updated CPUE standardization for the Spanish longline fleet targeting swordfish (*Xiphias gladius*) in the Southwest Pacific Ocean.

The most recent swordfish stock assessment for the Southwest Pacific was presented to the 17th Scientific Committee meeting of the Western and Central Pacific Fisheries Commission (WCPFC-SC17) in 2021 (Ducharme-Barth et al., 2021a). This assessment used data through 2019 and included standardized CPUE indices from multiple fleets. The Spanish fleet index (reported under European Union flag) was created using Vector Autoregressive Spatio-Temporal (VAST) models with delta-gamma modeling approaches applied to operational logbook data from 2004-2019 (Ducharme-Barth et al., 2021b).

1.1 Study Objectives

This analysis addresses three objectives for Spanish longline swordfish CPUE standardization:

1. Methodological Continuity: Maintain the base modeling framework from SC17 using delta-gamma (two-part) models to establish a consistent baseline for updating the index with additional data through 2023. Building upon the SC17 framework allows for direct extension of the existing time series while maintaining methodological consistency. The SC17 framework used spatiotemporal delta-generalized linear mixed models (GLMMs) within the VAST framework, employing binomial and gamma error distributions for the Spanish fleet (Ducharme-Barth et al., 2021b).

2. Alternative Modeling Approaches: Evaluate Tweedie models as an alternative to delta-gamma models. The Spanish longline fishery data exhibits very low zero-catch rates (0.5%), questioning the necessity of delta models that are specifically designed for zero-inflated data. Tweedie distributions provide a unified modeling framework that can handle both zero catches and positive continuous catches within a single model (Shono, 2008), eliminating the complexity of separate binomial and gamma components required by delta-gamma approaches. This single-component approach reduces the number of parameters to estimate compared to two-part models (Foster & Bravington, 2013). Three exploratory models investigate:

- M1: Baseline Tweedie model
- M2: Tweedie model with blue shark relative catch proportion covariate
- M3: Tweedie model with sea surface temperature covariate

3. Cross-Platform Validation: Implement alternative models (M1, M2, M3) across three software platforms to ensure computational robustness and validate implementation consistency. This includes VAST (Thorson, 2019), sdmTMB (Anderson et al., 2022), and tinyVAST (Thorson et al., 2025). Cross-platform implementation serves as a validation approach for model implementations and provides pathway options for future platform transitions, as all platforms utilize the Template Model Builder (TMB) computational backend (Kristensen et al., 2016) ensuring consistent underlying statistical computations.

2 Methods

2.1 Data and Study Area

The analysis utilized longline operational data from the Spanish longline fleet operating in the Southwest Pacific Ocean from 2004 to 2023, representing an update from the SC17 analysis which used data through 2019 (Ducharme-Barth et al., 2021a). The dataset was extracted from the Pacific Community (SPC) operational database following the same data extraction procedures and spatial boundaries as defined in SC17 (Ducharme-Barth et al., 2021b), but updated to include an additional four years (2020-2023) of observations.

The Spanish longline fishery operated across a broad area of the Southwest Pacific Ocean (Figure 1), with total annual fishing effort varying from approximately 2,000 to 4,000 sets per year (Figure 2). The spatial distribution of fishing sets showed notable changes over time, with operations contracting from broader eastern areas to concentrations near New Zealand waters (Figure 3). A significant shift in catch composition occurred from 2017 onwards when blue shark catches began exceeding swordfish catches, representing a major change in fishery dynamics (Figure 2).

Environmental covariates were incorporated from two sources: lunar phase calculated using the R oce package `moonAngle()` function (Kelley & Richards, 2023) to derive illuminated fraction values for each fishing operation; and sea surface temperature obtained from NOAA Optimum Interpolation Sea Surface Temperature (OISST) v2.1 daily high-resolution global grids (Huang et al., 2021) downloaded from NOAA Physical Sciences Laboratory (Figure 4). Blue shark (*Prionace glauca*) catch data from the same operational records served as a proxy for species interactions affecting swordfish catchability.

2.2 Base Model Framework

2.2.1 SC17 Continuity Model

The base model maintains the exact configuration used in SC17 to enable direct time series extension with data through 2023. Examination of the original SC17 analysis code confirmed the use of 100 spatial knots (Figure 5) and that the binomial component lacked spatiotemporal fields. Following the actual SC17 code implementation, the model employs:

- **Spatial configuration**: 100 spatial knots with fine-scale option disabled
- **Distribution**: Delta-gamma approach with binomial (encounter probability) and gamma (positive catch) components
- **Random effects**: Vessel random effects to account for catchability differences
- **Covariates**: Lunar phase effects on catchability using cubic B-splines
- **Platform**: VAST

Note: While the SC17 documentation (Ducharme-Barth et al., 2021b) indicated 200 knots and spatiotemporal effects in the binomial component, examination of the actual analysis code confirmed the implementation used 100 knots with no spatiotemporal effects in the binomial component.

The fine-scale disabled configuration uses piecewise constant spatial fields borrowing information from the nearest knots, exactly matching SC17 implementation. VAST's fine-scale setting (Thorson, 2019) controls spatial

interpolation: disabled (`fine_scale=FALSE`) uses piecewise constant fields at knot locations, while enabled (`fine_scale=TRUE`) applies bilinear interpolation across the spatial domain. Other platforms (sdmTMB and tinyVAST) use bilinear interpolation by default without fine-scale control options.

Additionally, the base model's delta-gamma structure requires different random effects specifications for the two linear predictors (encounter probability excludes spatiotemporal effects while positive catch includes them). VAST allows independent random effects configuration for each component, while sdmTMB requires identical spatial and spatiotemporal configurations across both components. tinyVAST supports independent configurations but lacks fine-scale options.

Base Model Formulas:

Encounter probability (binomial component):

```
Encounter ~ factor(YearQtr) + s(lunar, k=4) + (1|Vessel) + spatial
```

Positive catch rate (gamma component):

```
SWO_catch ~ factor(YearQtr) + s(lunar, k=4) + (1|Vessel) + spatial + spatiotemporal
```

where:

- `Encounter` : Binomial encounter probability (0/1)
- `SWO_catch` : Swordfish catch given encounter (kg)
- `factor(YearQtr)` : Fixed year-quarter effects
- `s(lunar, k=4)` : Smooth spline term for lunar phase effects (`k=4` specifies maximum 4 basis functions)
- `(1|Vessel)` : Random intercept for each vessel
- `spatial` : Spatial random field
- `spatiotemporal` : Spatiotemporal random field (gamma component only)

Model configuration: delta-gamma distribution, 100 spatial knots, fine-scale disabled, spatiotemporal effects turned off for encounter probability.

2.3 Exploratory Model Development

2.3.1 Alternative Distribution and Enhanced Spatial Resolution

Three exploratory models using Tweedie distributions were developed because the Spanish longline fishery data exhibits very low zero-catch rates (0.5%), questioning the necessity of delta models that are specifically designed for zero-inflated data. Tweedie distributions provide a unified modeling framework that can handle both zero catches and positive continuous catches within a single model (Shono, 2008), eliminating the complexity of separate binomial and gamma components required by delta-gamma approaches. This single-component approach reduces the number of parameters to estimate compared to two-part models (Foster & Bravington, 2013), reducing model complexity and parameter estimation uncertainty while maintaining distributional flexibility.

These models employed 200 spatial knots (Figure 5) with fine-scale option enabled for improved spatial resolution. Unlike the base model where spatiotemporal effects were limited to the gamma component only, all Tweedie models included spatiotemporal random effects alongside spatial effects for the unified response. Spatiotemporal modeling

can capture time-varying spatial patterns in species distribution (Thorson et al., 2015) and may improve precision by borrowing strength across space and time (Shelton et al., 2014). This approach may be particularly beneficial for mobile pelagic species in dynamic oceanic environments (Thorson, 2019).

2.3.2 Environmental and Biological Covariates

Sea Surface Temperature (SST): Quarterly 1-degree resolution data obtained from NOAA OISST (Huang et al., 2021) to capture thermal habitat preferences. Temperature is included as an environmental covariate given that swordfish are highly mobile pelagic species that may respond to thermal gradients in oceanic environments (Sepulveda et al., 2010).

Blue Shark Relative Catch Proportion (BSH_logit): Logit-transformed proportion representing potential species interactions that may affect swordfish catchability.

2.3.3 Model Specifications

M1: Baseline Tweedie - SC17 framework with Tweedie distribution (instead of delta-gamma):

```
SWO_catch ~ factor(YearQtr) + s(lunar, k=4) + (1|Vessel)+ spatial + spatiotemporal
```

M2: Blue Shark Interaction - M1 + blue shark relative catch proportion covariate:

```
SWO_catch ~ factor(YearQtr) + s(lunar, k=4) + (1|Vessel) + BSH_logit + spatial + spatiotemporal
```

M3: Environmental Temperature - M1 + sea surface temperature covariate:

```
SWO_catch ~ factor(YearQtr) + s(lunar, k=4) + (1|Vessel) + s(SST, k=4) + spatial + spatiotemporal
```

where:

- `BSH_logit` : Logit-transformed blue shark relative catch proportion
- `s(SST, k=4)` : Smooth spline term for sea surface temperature

Note: A fourth model (M4) combining both blue shark and SST covariates was considered but excluded due to convergence issues across all platforms.

These exploratory models employed 200 spatial knots with fine-scale option enabled for improved spatial resolution, contrasting with the Base model's 100 knots configuration.

2.4 Cross-Platform Implementation

The base model was implemented in VAST only due to platform-specific requirements: fine-scale disabled option (unavailable in sdmTMB and tinyVAST) and independent random effects configuration for delta components (sdmTMB requires identical configurations across both linear predictors). All exploratory models (M1, M2, M3) were implemented across VAST (Thorson, 2019), sdmTMB (Anderson et al., 2022), and tinyVAST (Thorson et al., 2025) for implementation validation and future platform transitions.

2.5 Model Diagnostics and Selection

2.5.1 Convergence Assessment

Convergence was verified using standard criteria: maximum gradient <1e-6, successful optimizer exit, and positive definite Hessian matrix. Parameter standard errors were examined for unreasonably large values indicating numerical instability. The sdmTMB platform provided automated diagnostics via `sanity()` checks for convergence status, Hessian matrix properties, eigenvalue extremes, gradient magnitudes, and parameter validity.

2.5.2 Model Adequacy and Comparison

Model adequacy was assessed using probability integral transform (PIT) residuals (Dunn & Smyth, 1996) via Q-Q plots and residuals versus fitted values to detect distributional misspecification and systematic patterns. Q-Q plots evaluate distributional assumptions by comparing PIT residuals against theoretical uniform distribution quantiles, with deviations indicating distributional misspecification. Residuals versus fitted plots assess structural adequacy by examining systematic prediction bias through LOESS (locally estimated scatterplot smoothing) curves, with patterns indicating model structural inadequacy. Spatial distribution of residuals was also examined to identify systematic spatial bias.

Model comparison among M1, M2, and M3 used marginal likelihood-based AIC (Akaike, 1974). This approach is known to be effective when comparing models with identical random effects structures (Auger-Méthé et al., 2021; Kim et al., 2024). Since all three exploratory models share the same random effects configuration (vessel, spatial, and spatiotemporal effects), marginal likelihood-based AIC was used for model selection. Cross-platform validation ensured computational consistency across implementations.

3 Results

3.1 Model Convergence and Cross-Platform Validation

All four models achieved successful convergence. Cross-platform validation of exploratory models M1, M2, and M3 demonstrated identical results across VAST, sdmTMB, and tinyVAST implementations (Figure 6), confirming computational consistency and reproducibility.

3.2 Model Diagnostic Analysis

Model diagnostics revealed significant differences in performance across the four models (Figure 7). The Base model (Delta-Gamma) showed notable deviations from uniform distribution in Q-Q plots and systematic curved patterns in residuals versus fitted values, indicating both distributional and structural inadequacies. M1 (Tweedie baseline) demonstrated marked improvement with good adherence to uniform distribution and relatively flat residuals. M2 (Tweedie + Blue Shark) exhibited good distributional fit similar to M1, but showed more pronounced curvature in residual patterns. M3 (Tweedie + SST) displayed optimal performance with good alignment to uniform distribution and flat residuals similar to M1.

Spatial residual patterns (Figure 8) revealed that all four models displayed relatively random spatial distributions without systematic bias.

3.3 Model Selection and Covariate Effects

Model comparison using AIC showed substantial differences among the exploratory Tweedie models (Table 1). M2 (blue shark covariate) achieved the lowest AIC, followed by M3 (SST covariate) and M1 (baseline). The AIC differences were large: M2 had the best fit, with M3 showing ΔAIC = 3789.3 and M1 showing ΔAIC = 3832.1, indicating that covariate inclusion substantially improved model fit.

However, AIC rankings and diagnostic performance showed important trade-offs. While M2 had the best statistical fit, it exhibited more residual curvature compared to M1 and M3. M3 demonstrated the optimal balance between statistical fit and diagnostic adequacy, suggesting that environmental covariates (SST) provide meaningful predictive value while maintaining model adequacy.

3.4 CPUE Index Trends

Standardized CPUE indices showed similar trends across all models (Figure 9 and Figure 10). All models demonstrated fluctuating patterns from 2004 to 2021, followed by a sharp decline from 2022 onwards. The overall temporal patterns were largely comparable among models, indicating robust trend estimation regardless of model choice.

3.5 Spatial Predictions

Annual density predictions showed generally consistent spatial patterns across all models (Figure 11-Figure 14), with no major differences in overall distribution. The Base model displayed discrete spatial predictions at knot locations due to its fine-scale disabled configuration, while Tweedie models showed smooth interpolation. The main spatial pattern showed swordfish density concentrated in two primary areas: near New Zealand waters and the northern region boundary. However, recent years (2022-2023) showed a shift with density concentrations primarily limited to the New Zealand region.

4 Discussion

4.1 Model Performance and Selection

Tweedie models proved computationally robust for this dataset with minimal zero catches (0.5%), while delta-gamma approaches encountered convergence difficulties when finer spatial resolution and additional covariates were applied. The delta-gamma model's convergence issues highlight the challenges of using this approach for datasets with low zero catch rates, as it relies on a more complex structure that may not be necessary for such data.

Despite M2 achieving the lowest AIC (Table 1), its systematic residual patterns indicated that blue shark proxies may not adequately capture underlying mechanisms affecting swordfish catchability. SST covariates provided better structural model performance than blue shark proxies, though both improved statistical fit. The similar diagnostic quality between baseline and SST models suggests environmental covariates offer meaningful but modest improvements.

The observed spatiotemporal changes in fishing operations raise fundamental questions about data suitability as potential indices of swordfish abundance. The spatial contraction of fishing effort coincided with increased blue shark catches from 2017 onwards, suggesting that fishing operations concentrated in blue shark-dominated areas. This raises concerns that the spatial predictions may reflect operational changes rather than true swordfish distribution patterns.

4.2 Limitations and Uncertainties

None of the covariate models fully explained recent CPUE declines, suggesting additional factors beyond those examined. Without detailed targeting information, the underlying drivers of these trends remain unclear. This uncertainty affects the reliability of these indices for stock assessment purposes.

Cross-platform validation confirmed computational consistency across VAST, sdmTMB, and tinyVAST, supporting future transitions to more accessible platforms.

4.3 Recommendations

Given the limitations in explaining recent CPUE trends, the SC17 base model structure was maintained for continuity. Future analyses should explore Tweedie distributions for datasets with minimal zero catches and consider transitioning to more accessible platforms like sdmTMB or tinyVAST.

Better targeting information is essential to distinguish between abundance changes and operational shifts. Additional covariates may be needed to capture the factors driving recent CPUE patterns in the Southwest Pacific longline fishery.

5 Conclusions

This analysis maintained SC17 continuity while exploring alternative modeling approaches for Spanish longline CPUE standardization. Tweedie models proved more robust than delta-gamma approaches for this dataset with minimal zero catches (0.5%), particularly when incorporating environmental covariates and finer spatial resolution.

Both SST and blue shark covariates showed statistical significance, though neither M2 nor M3 fully explained recent CPUE declines. M3 performed best among the exploratory models, suggesting climate factors may improve CPUE standardization. However, the inability to explain recent trends highlights the need for better longline targeting information and additional covariates.

Cross-platform validation across VAST, sdmTMB, and tinyVAST confirmed computational consistency and supports future transitions as VAST is replaced by tinyVAST. We recommend M3 as a foundation for future CPUE analysis, though the unclear causes of recent CPUE drops could introduce bias if these indices are used directly in stock assessments without resolving whether the declines reflect genuine abundance changes or shifts in targeting behavior.

Acknowledgments

We thank Nicholas Ducharme-Barth (NOAA) for providing detailed explanations of the previous SC17 swordfish CPUE analysis methodology and for sharing the Quarto template used for this report. We also thank the Stock Assessment Modelling Team of the Oceanic Fisheries Programme for valuable discussions that contributed to this analysis.

References

Akaike, H. (1974). A new look at the statistical model identification. *IEEE Transactions on Automatic Control*, *19*(6), 716–723. https://doi.org/10.1109/TAC.1974.1100705

Anderson, S. C., Ward, E. J., English, P. A., & Barnett, L. A. K. (2022). sdmTMB: An R package for fast, flexible, and user-friendly generalized linear mixed effects models with spatial and spatiotemporal random fields. *bioRxiv*. https://doi.org/10.1101/2022.03.24.485545

Auger-Méthé, M., Newman, K., Cole, D., Empacher, F., Gryba, R., King, A. A., Leos-Barajas, V., Mills Flemming, J., Nielsen, A., Petris, G., & Thomas, L. (2021). A guide to state–space modeling of ecological time series. *Ecological Monographs*, *91*(4), e01470. https://doi.org/10.1002/ecm.1470

Ducharme-Barth, N., Castillo-Jordán, C., Hampton, J., Williams, P., Pilling, G., & Hamer, P. (2021a). *Stock assessment of southwest Pacific swordfish* (WCPFC-SC17-2021/SA-WP-04). Western and Central Pacific Fisheries Commission.

Ducharme-Barth, N., Peatman, T., & Hamer, P. (2021b). *Background analyses for the 2021 stock assessment of Southwest Pacific swordfish* (WCPFC-SC17-2021/SA-IP-07). Western and Central Pacific Fisheries Commission.

Dunn, P. K., & Smyth, G. K. (1996). Randomized quantile residuals. *Journal of Computational and Graphical Statistics*, *5*(3), 236–244. https://doi.org/10.1080/10618600.1996.10474708

Foster, S. D., & Bravington, M. V. (2013). A Poisson–gamma model for analysis of ecological non-negative continuous data. *Environmental and Ecological Statistics*, *20*(4), 533–552. https://doi.org/10.1007/s10651-012-0233-0

Huang, B., Liu, C., Banzon, V., Freeman, E., Graham, G., Hankins, B., Smith, T., & Zhang, H.-M. (2021). NOAA 0.25-degree daily Optimum Interpolation Sea Surface Temperature (OISST), version 2.1. *NOAA National Centers for Environmental Information*. https://doi.org/10.25921/RE9P-PT57

Kelley, D., & Richards, C. (2023). *oce: Analysis of Oceanographic Data*. https://CRAN.R-project.org/package=oce

Kim, K., Sibanda, N., Arnold, R., & A'mar, T. (2024). Enhancing data-limited assessments with random effects: A case study on Korea chub mackerel (*Scomber japonicus*). *Canadian Journal of Fisheries and Aquatic Sciences*, *81*(12), 1768–1784. https://doi.org/10.1139/cjfas-2023-0358

Kristensen, K., Nielsen, A., Berg, C. W., Skaug, H., & Bell, B. M. (2016). TMB: Automatic Differentiation and Laplace Approximation. *Journal of Statistical Software*, *70*(5), 1–21. https://doi.org/10.18637/jss.v070.i05

Maunder, M. N., & Punt, A. E. (2004). Standardizing catch and effort data: A review of recent approaches. *Fisheries Research*, *70*(2-3), 141–159. https://doi.org/10.1016/j.fishres.2004.08.002

Sepulveda, C. A., Knight, A., Nasby-Lucas, N., & Domeier, M. L. (2010). Fine-scale movements of the swordfish Xiphias gladius in the Southern California Bight. *Fisheries Oceanography*, *19*(4), 279–289. https://doi.org/10.1111/j.1365-2419.2010.00543.x

Shelton, A. O., Thorson, J. T., Ward, E. J., & Feist, B. E. (2014). Spatial semiparametric models improve estimates of species abundance and distribution. *Canadian Journal of Fisheries and Aquatic Sciences*, *71*(11), 1655–1666. https://doi.org/10.1139/cjfas-2013-0508

Shono, H. (2008). Application of the Tweedie distribution to zero-catch data in CPUE analysis. *Fisheries Research*, *93*(1-2), 154–162. https://doi.org/10.1016/j.fishres.2008.03.006

Thorson, J. T. (2019). Guidance for decisions using the Vector Autoregressive Spatio-Temporal (VAST) package in stock, ecosystem, habitat and climate assessments. *Fisheries Research*, *210*, 143–161. https://doi.org/10.1016/j.fishres.2018.10.013

Thorson, J. T., Anderson, S. C., Goddard, P., & Rooper, C. N. (2025). tinyVAST: R package with an expressive interface to specify lagged and simultaneous effects in multivariate spatio-temporal models. *Global Ecology and Biogeography*, *34*(4), e70035. https://doi.org/10.1111/geb.70035

Thorson, J. T., Shelton, A. O., Ward, E. J., & Skaug, H. J. (2015). Geostatistical delta-generalized linear mixed models improve precision for estimated abundance indices for West Coast groundfishes. *ICES Journal of Marine Science*, *72*(5), 1297–1310. https://doi.org/10.1093/icesjms/fsu243

Table 1: Comparison of exploratory Tweedie models showing AIC values, delta AIC (difference from lowest AIC value), and number of estimated parameters. All models include spatial and spatiotemporal random effects with 200 spatial knots.

Model	Description	AIC	Δ AIC	Parameters
M1	Baseline Tweedie (SC17 covariates)	398784.7	3832.1	89
M2	M1 + Blue shark catch proportion	394952.6	0.0	90
M3	M1 + Sea surface temperature	398741.9	3789.3	92

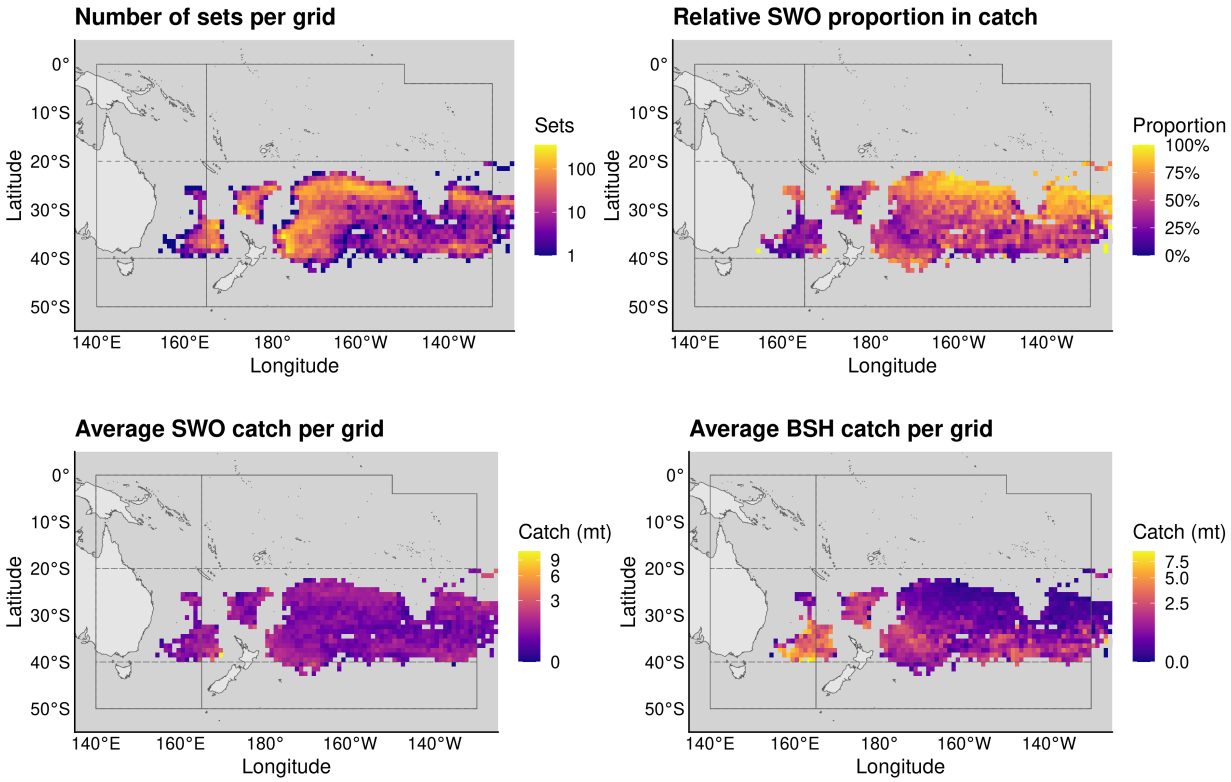

Figure 1: Spatial distribution of Spanish longline fishing operations in the Southwest Pacific Ocean (2004-2023). Top left: Number of longline sets per 1° grid cell. Top right: Relative proportion of swordfish in total catch by grid cell. Bottom left: Average swordfish catch per grid cell in metric tonnes. Bottom right: Average blue shark catch per grid cell in metric tonnes.

Figure 2: Annual time series of Spanish longline fishing operations (2004-2023). Blue bars show total number of longline sets per year. Red and green lines represent annual catches in metric tonnes for swordfish and blue shark, respectively. Data for 2004 exclude first and second quarters, resulting in lower values for that year.

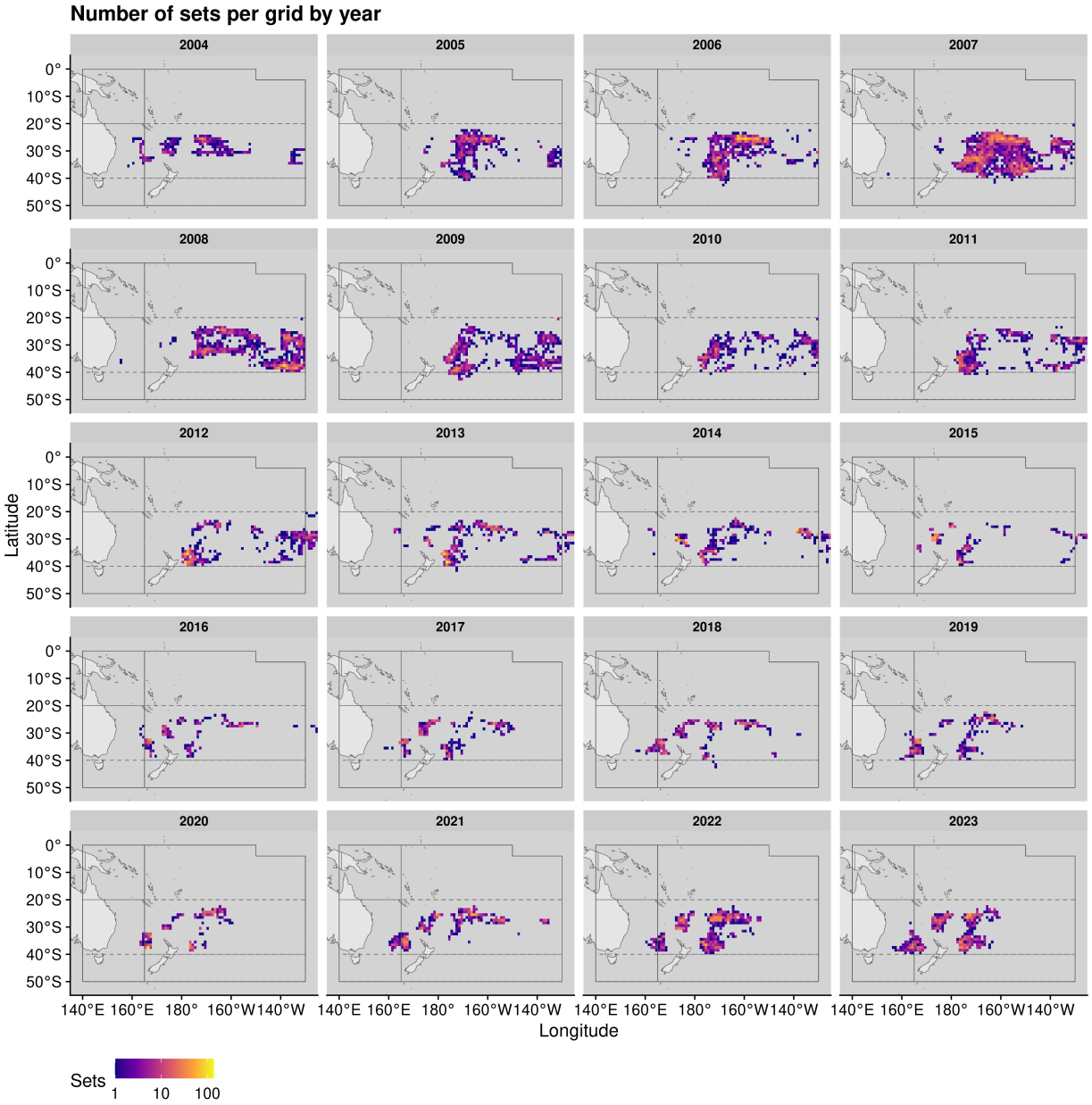

Figure 3: Annual spatial distribution of Spanish longline sets from 2004-2023.

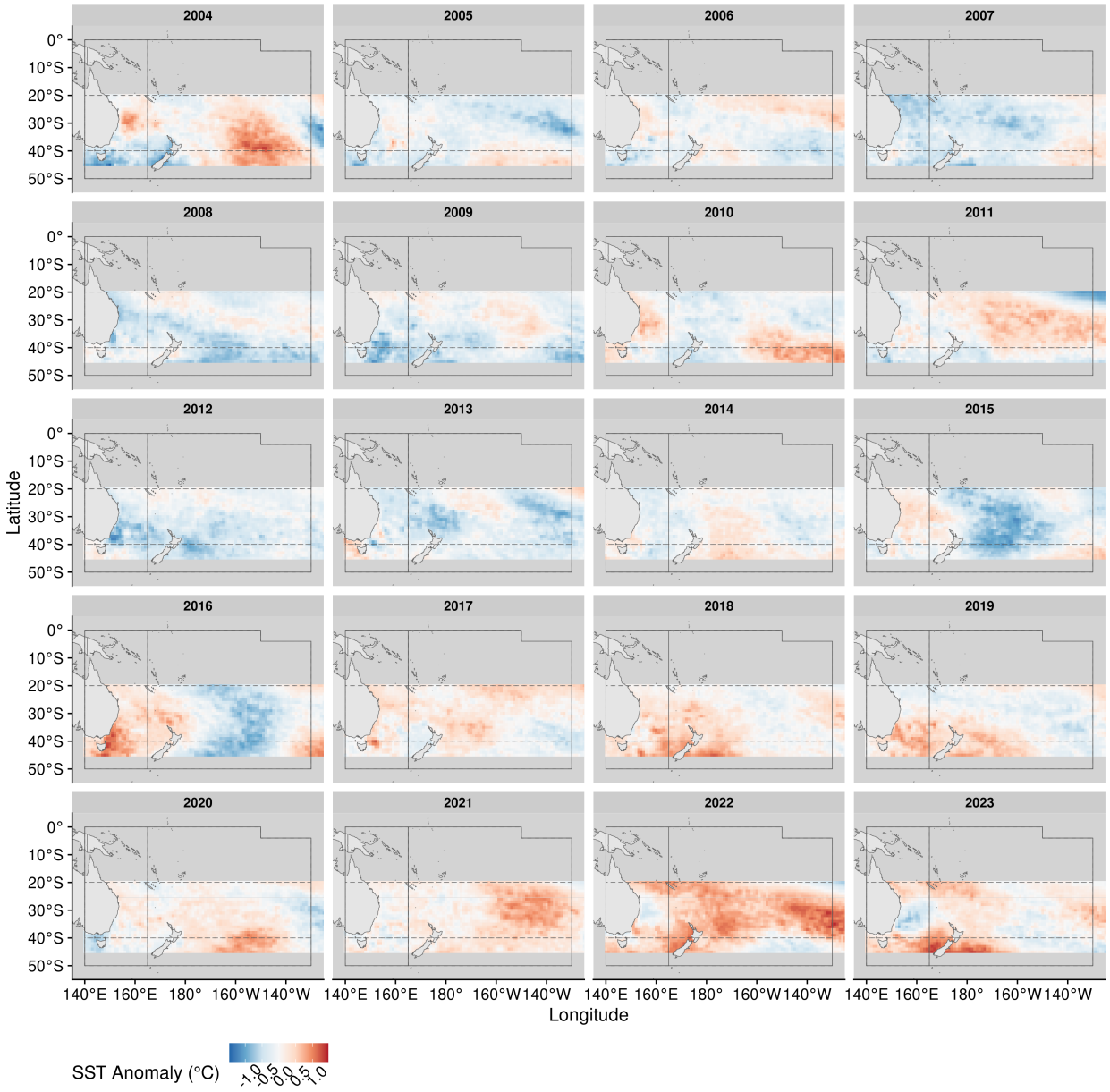

Figure 4: Annual spatial distribution of sea surface temperature anomalies from 2004-2023 across the Southwest Pacific study area.

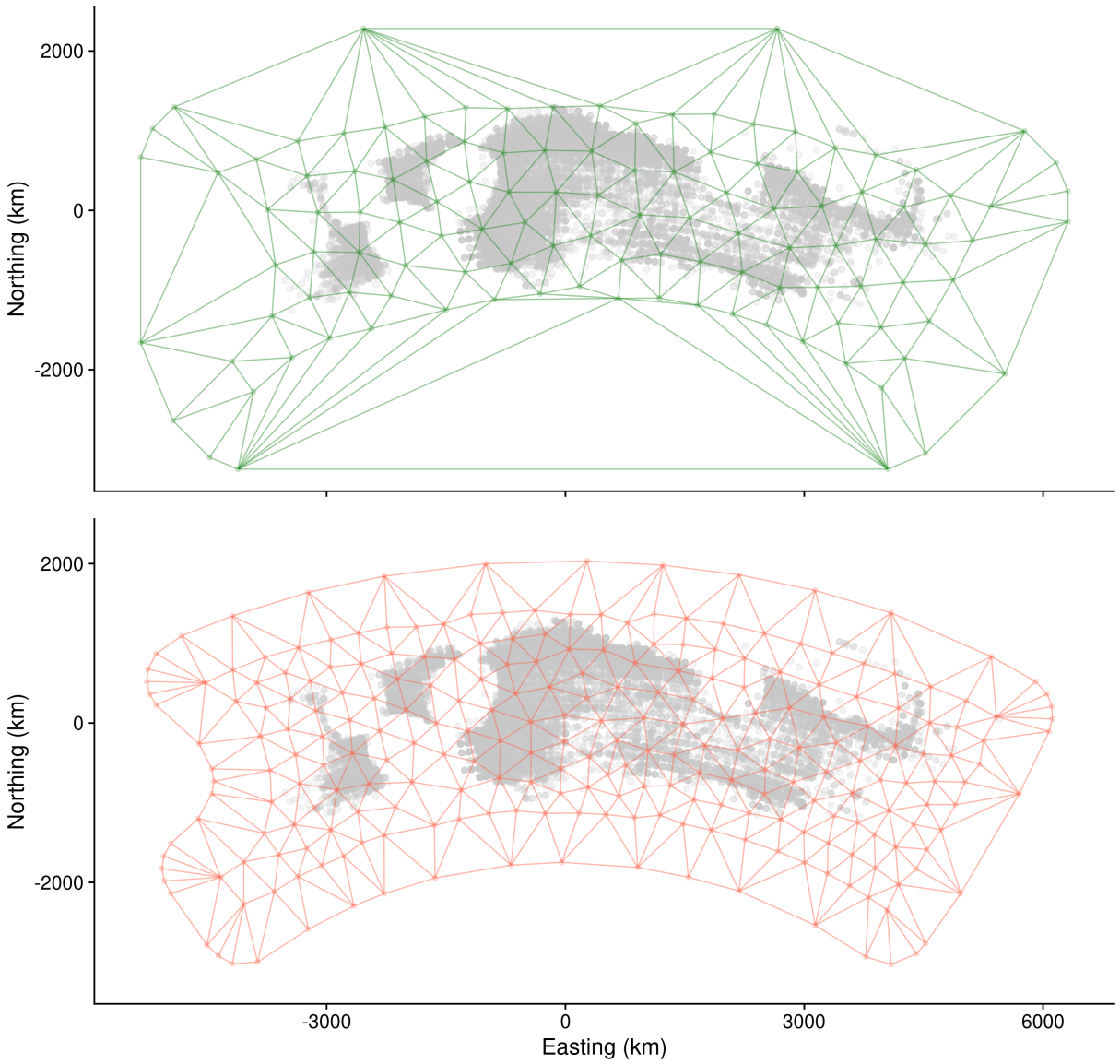

Figure 5: Spatial mesh configurations used in the analysis. Top panel: 100 knots (Base model) with green mesh lines. Bottom panel: 200 knots (exploratory Tweedie models M1, M2, M3) with coral-colored mesh lines. Grey points represent fishing operation data locations. Knots define spatial random field structure across the Southwest Pacific study area, with coordinates in projected coordinate system (kilometers).

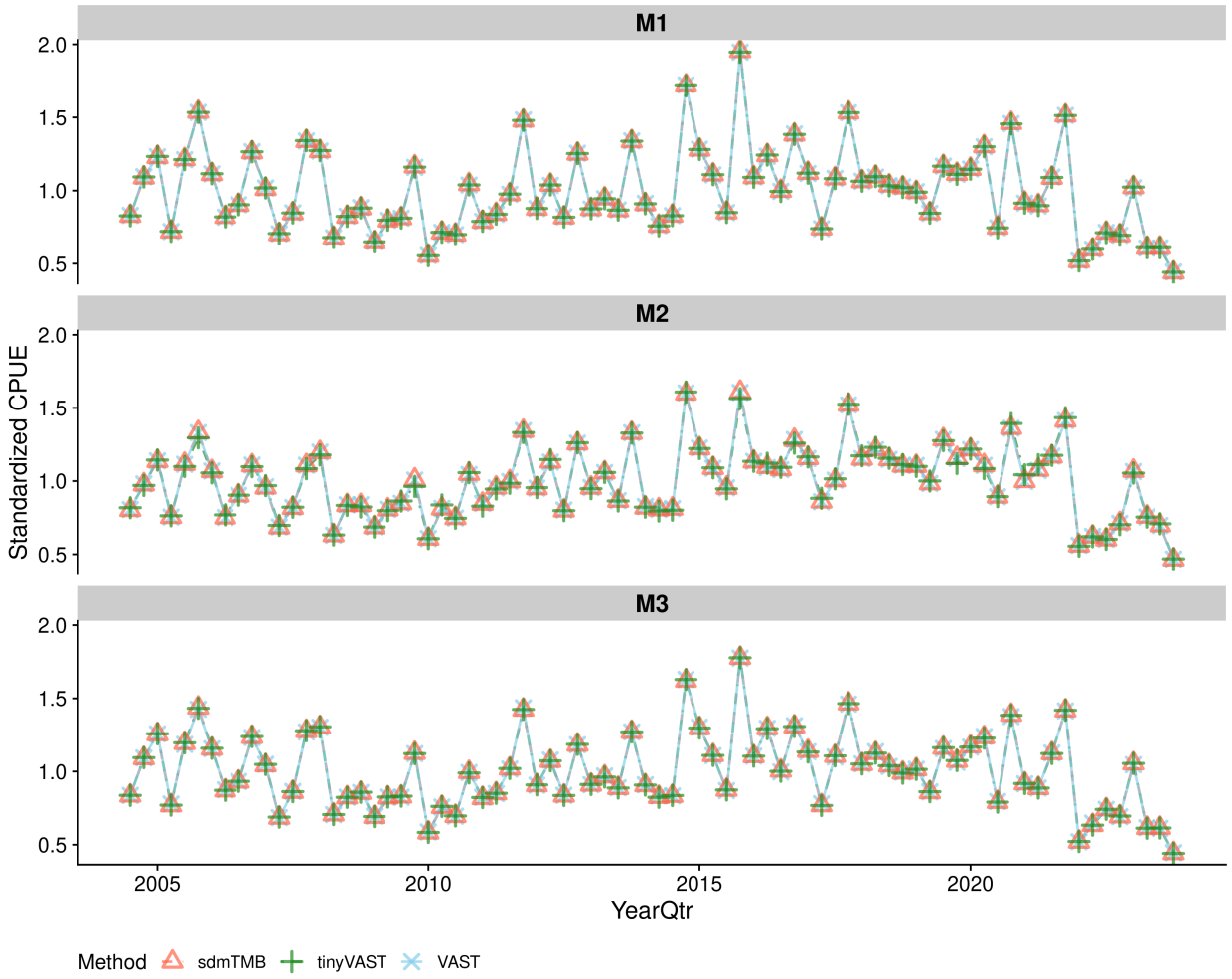

Figure 6: Cross-platform validation showing identical standardized CPUE indices across three software implementations. Three panels show models M1, M2, and M3 with VAST (sky blue, asterisks), sdmTMB (coral, triangles), and tinyVAST (green, crosses). Overlapping symbols demonstrate perfect computational agreement between platforms.

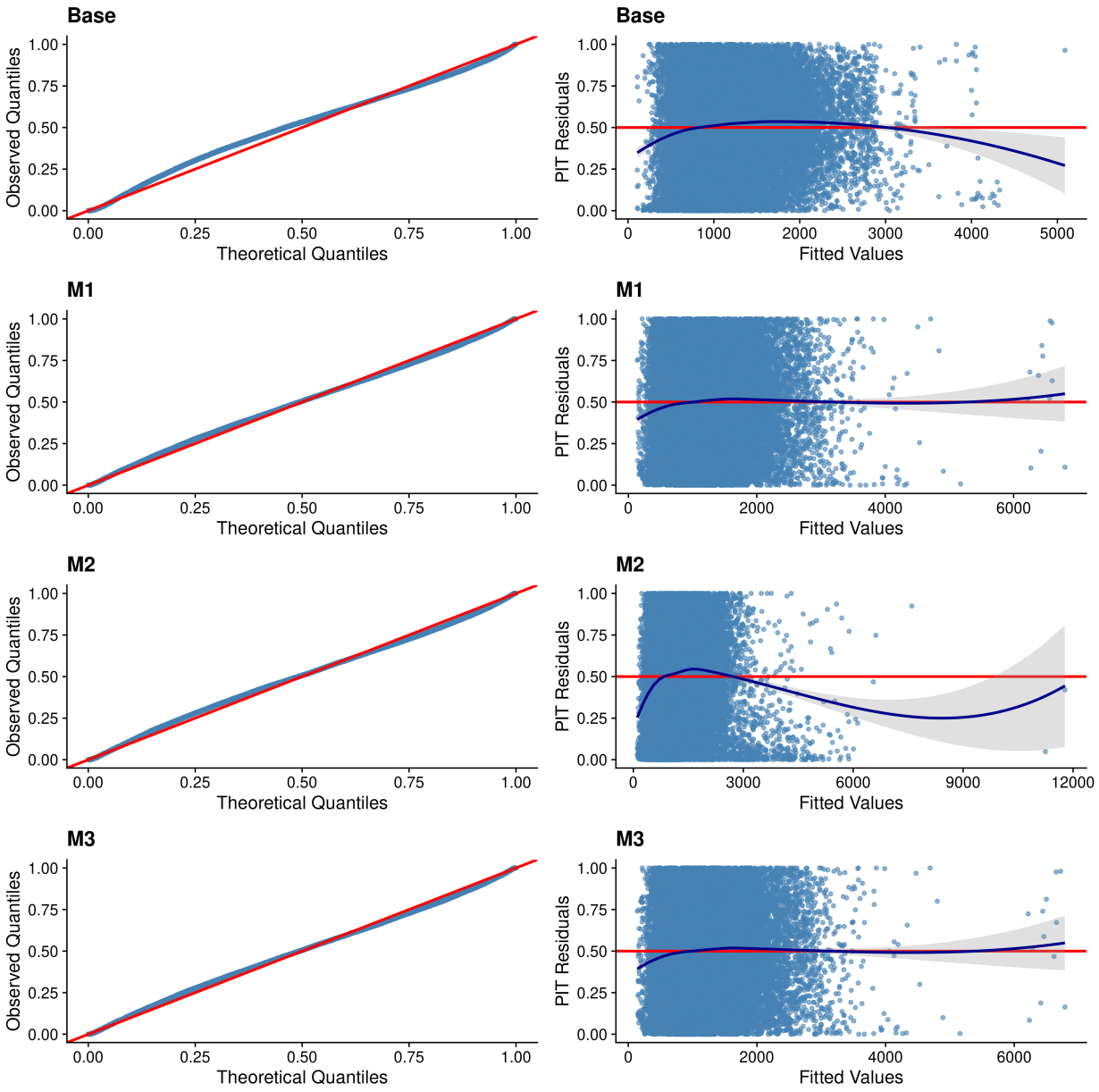

Figure 7: Model diagnostic plots for all four models (Base, M1, M2, M3) arranged in 4 rows. Left column: Q-Q plots comparing PIT residuals (dots) against theoretical uniform distribution (diagonal line). Right column: Residuals versus fitted values with LOESS curves (blue lines).

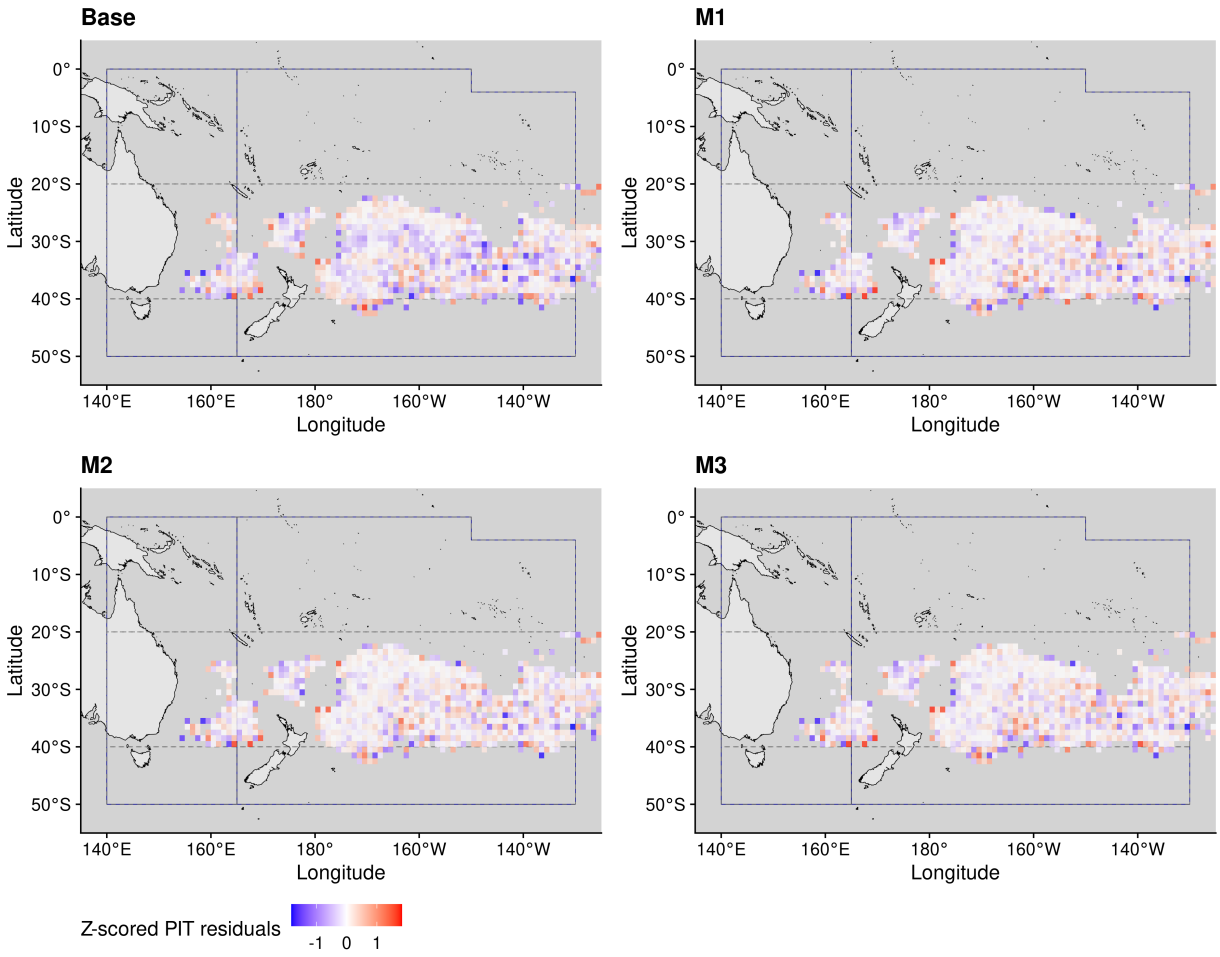

Figure 8: Spatial distribution of z-scored PIT residuals for all four models arranged in 4 panels (Base, M1, M2, M3) from top to bottom order. Blue-red color scale with white indicating good fit (residuals near zero).

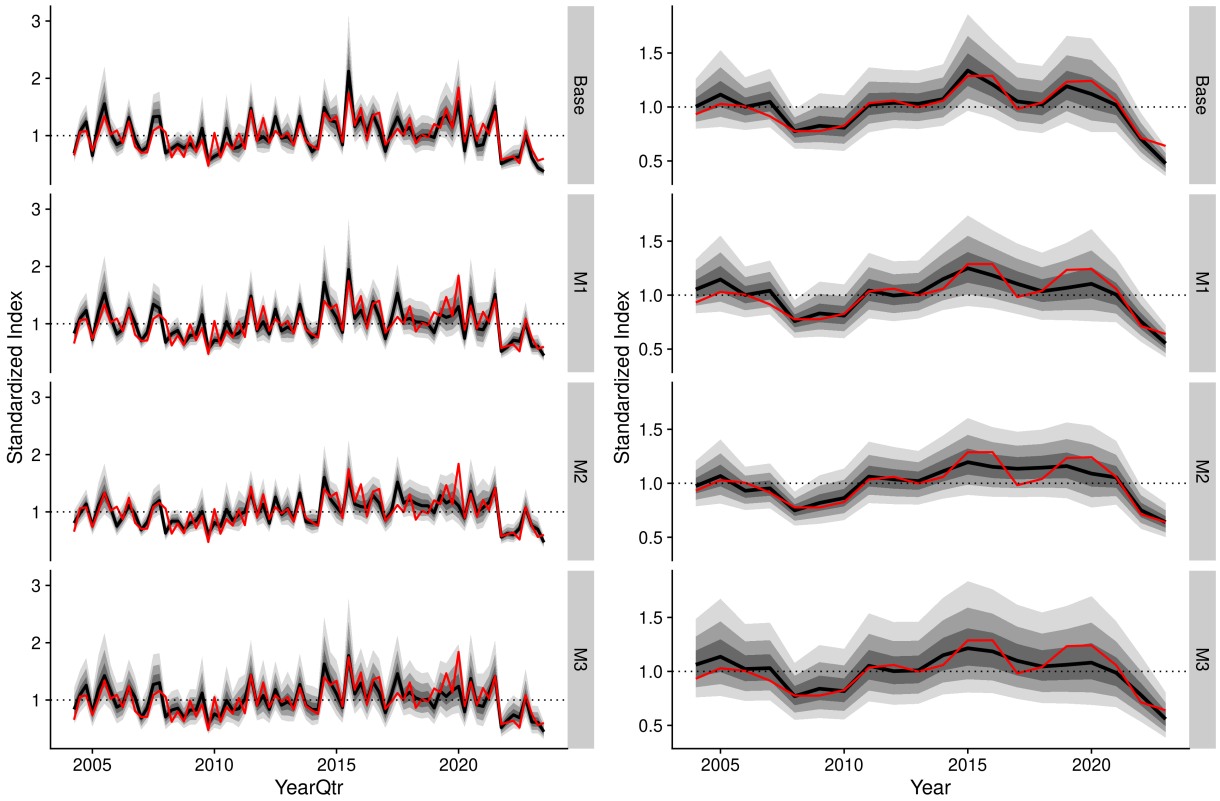

Figure 9: Comparison of standardized CPUE indices from four models. Left panels: Quarterly indices (2004-2023). Right panels: Annual indices (2004-2023). Black lines show point estimates with grey uncertainty bands (50%, 80%, 95% confidence intervals). Red lines represent nominal CPUE. All indices scaled to mean = 1.

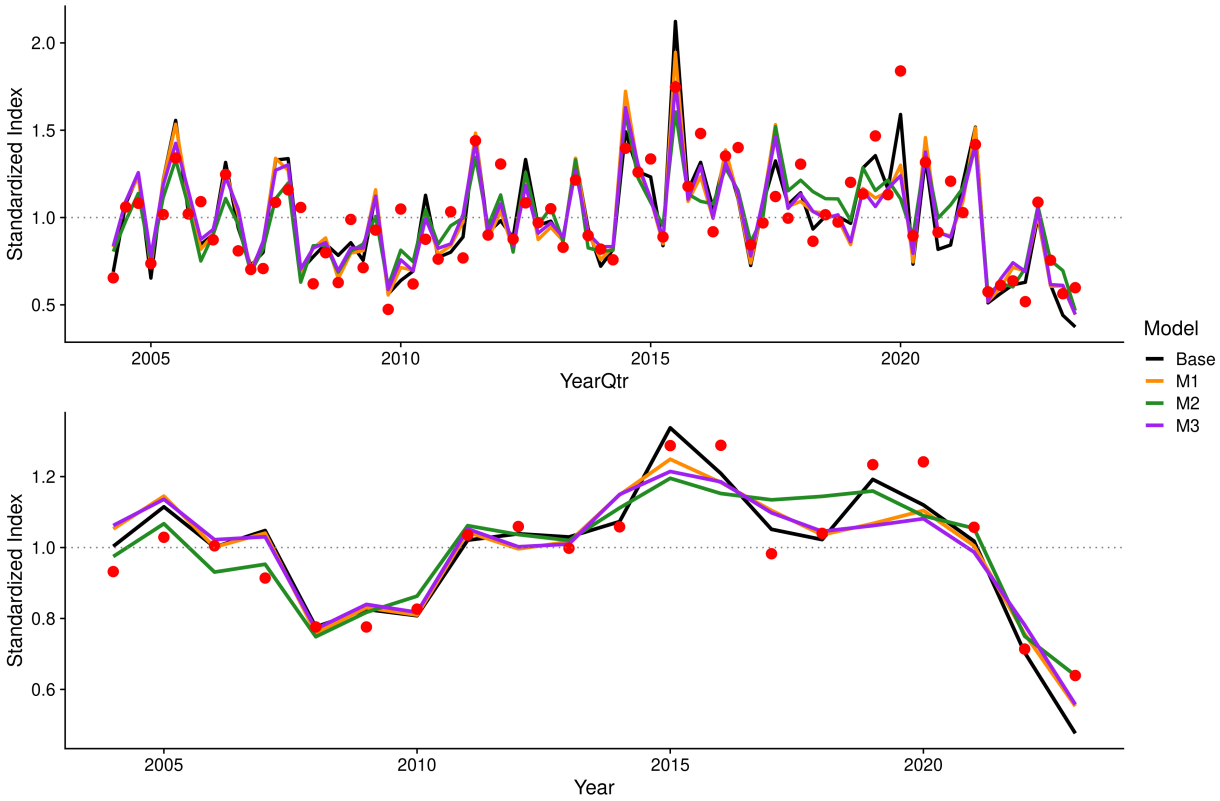

Figure 10: Standardized CPUE indices from four models (2004-2023). Top panel: Quarterly indices. Bottom panel: Annual indices. Base model (black line), M1 (orange line), M2 (green line), M3 (purple line), and nominal CPUE (red points). Indices scaled to mean = 1.

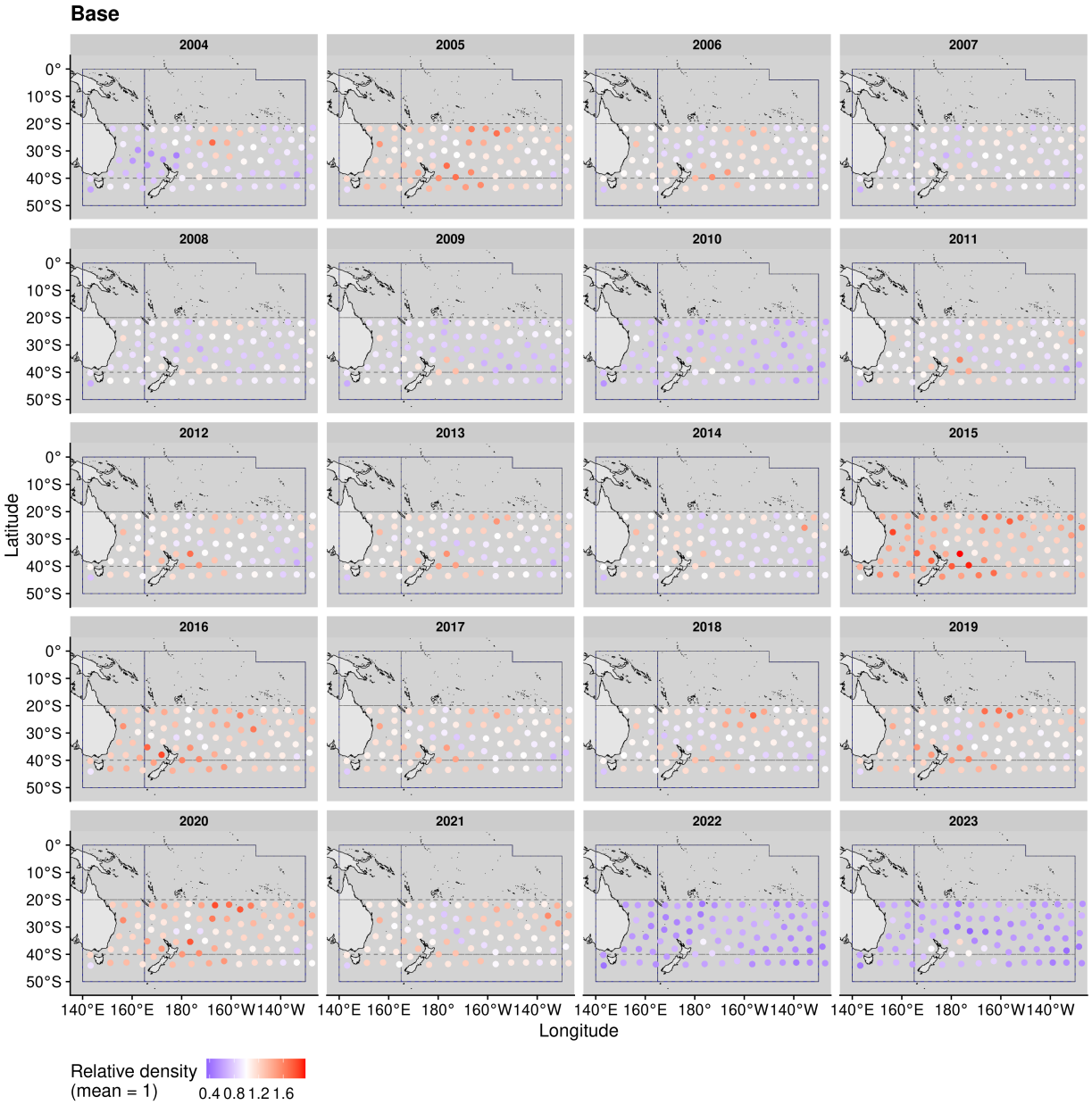

Figure 11: Annual spatial predictions of relative swordfish density from Base model (delta-gamma) 2004-2023.

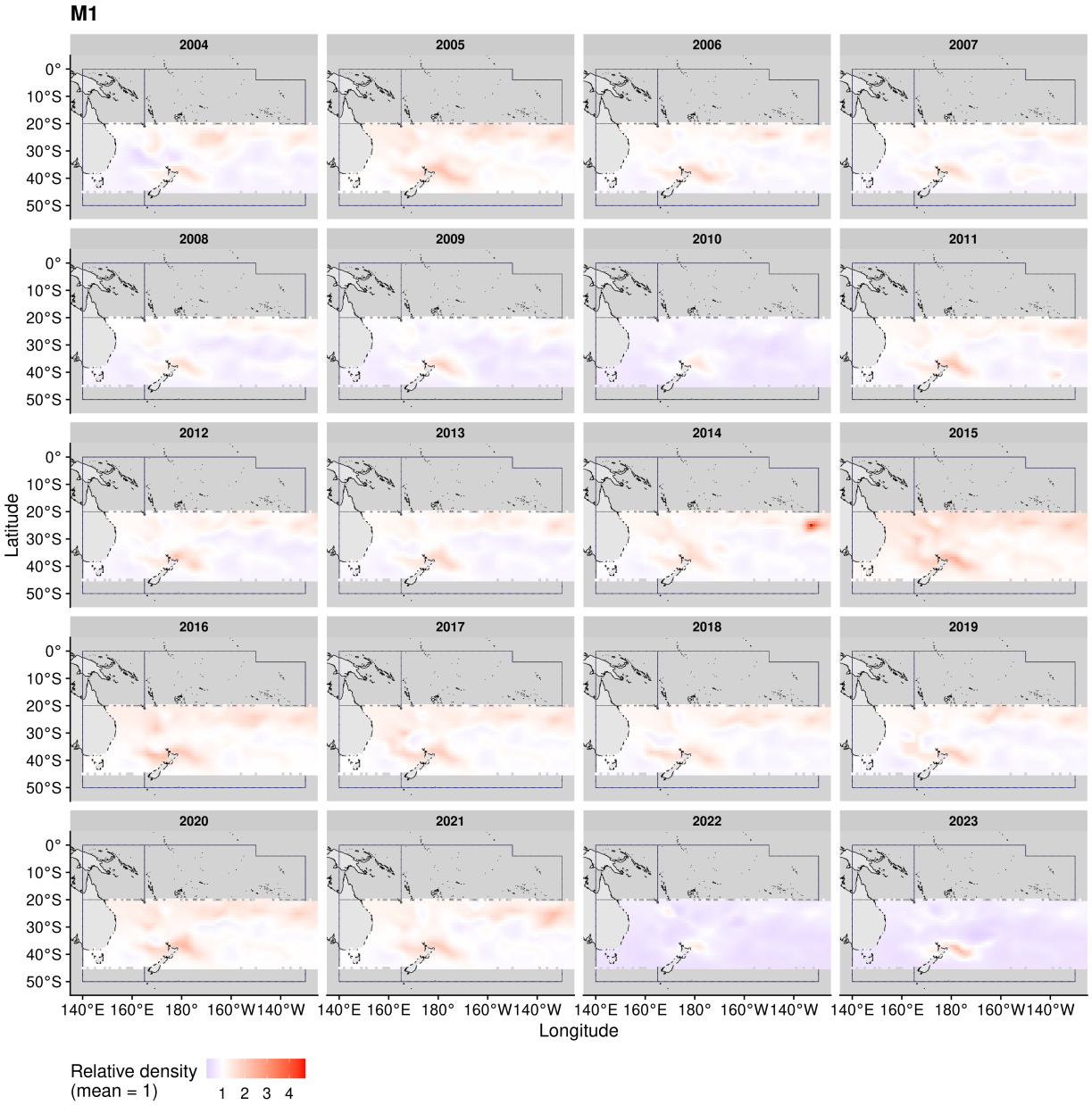

Figure 12: Annual spatial predictions of relative swordfish density from Model M1 (Tweedie baseline) 2004-2023.

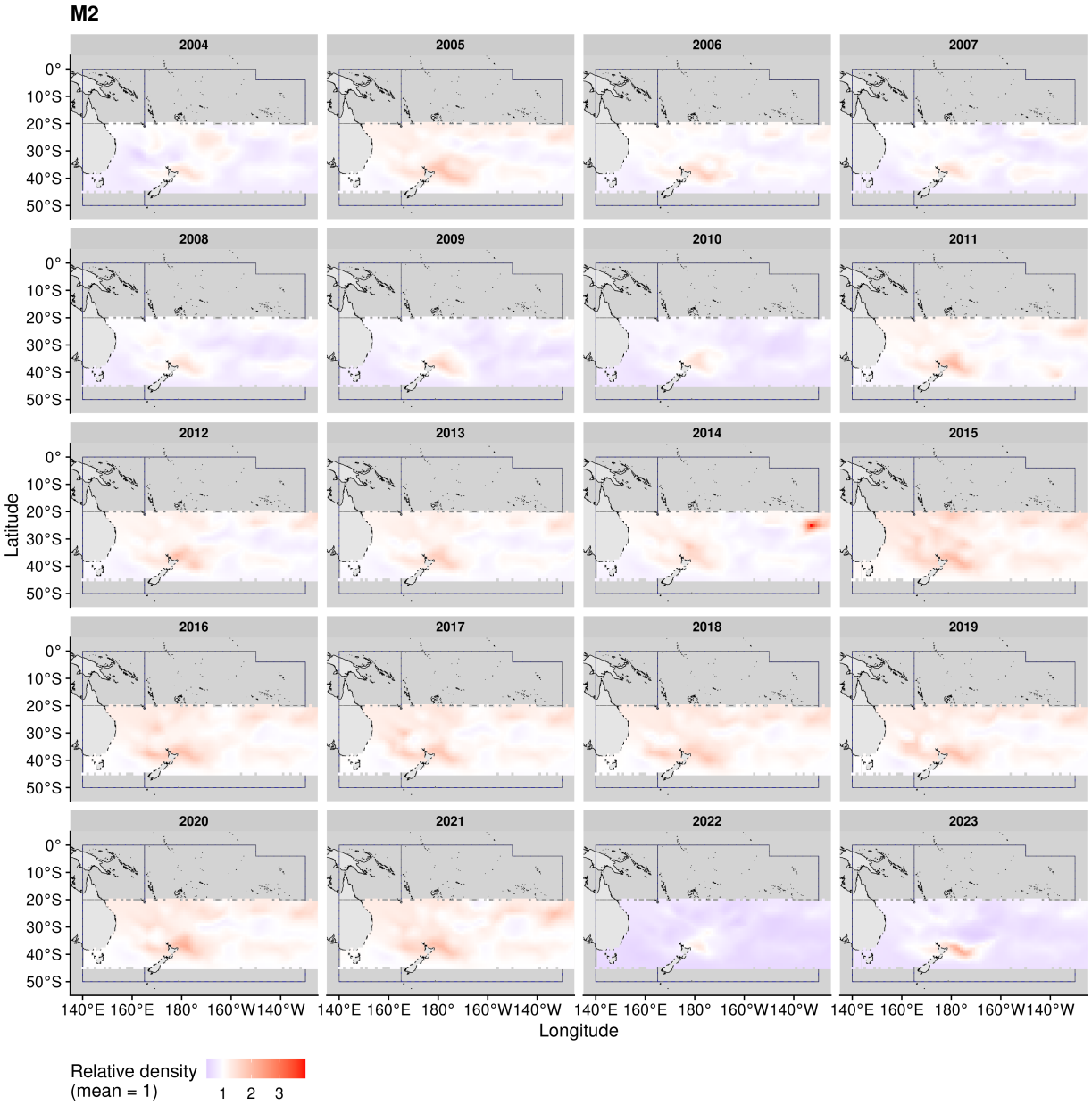

Figure 13: Annual spatial predictions of relative swordfish density from Model M2 (Tweedie + blue shark covariate) 2004-2023.

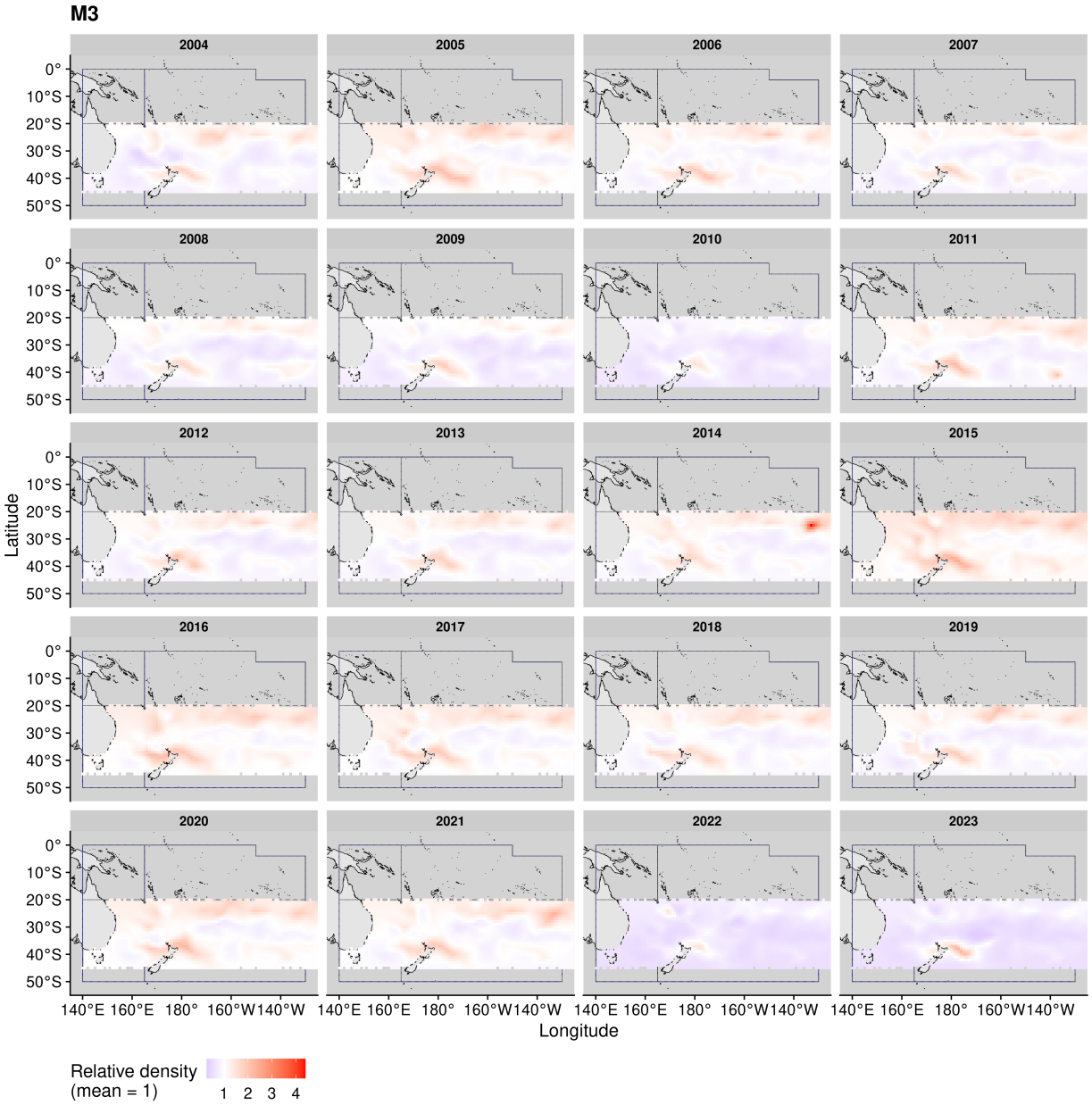

Figure 14: Annual spatial predictions of relative swordfish density from Model M3 (Tweedie + SST covariate) 2004-2023.